African Journal of Biotechnology Vol. 10(76), pp. 17551-17563, 30 November, 2011
Available online at http://www.academicjournals.org/AJB
DOI: 10.5897/AJB10.2558
ISSN 1684–5315 © 2011 Academic Journals

Full Length Research Paper

Proteomic analysis of the *Arabidopsis thaliana*-*Botrytis cinerea* interaction using two-dimensional liquid chromatography

Joseph M. K. Mulema[1,4]*, Patrick Okori[2] and Katherine J. Denby[1,3]

[1]Department of Molecular and Cell Biology, University of Cape Town, Private Bag 7701 Rondebosch, South Africa.
[2]Department of Agricultural Production, School of Agricultural Sciences, College of Agricultural and Environmental Sciences, Makerere University, P.O. Box 7062, Kampala, Uganda.
[3]School of Life Sciences and Warwick Systems Biology Centre, University of Warwick, Wellesbourne Campus, Wellesbourne, Warwick, CV35 9EF, United Kingdom.
[4]CABI Africa, ICRAF Complex, United Nations Avenue, Gigiri, PO Box 633-00621, Nairobi, Kenya.

Accepted 27 October, 2011

A two-dimensional liquid chromatography (2D LC) system, ProteomeLab PF 2D, was employed to study the defence proteome of Arabidopsis following infection with the necrotrophic fungal pathogen, *Botrytis cinerea*. This system demonstrated differential protein expression in control and treated samples in some fractions. However, the amount of proteins in the fractions and the level to which they were changing could not be established. Among the proteins identified in the fractions that displayed an increase in absorbance was catalase 3 and glutathione S-transferases, demonstrating the importance of an antioxidant system in defence against *B. cinerea*. Most of the proteins were identified in fractions that displayed reduction in absorbance. Functional categorisation of the identified proteins demonstrated the overrepresentation of photosynthetic pathway, a phenomenon also observed in other host and nonhost pathogen interactions. Proteomelab PF 2D did not identify as many proteins as expected possibly due to the masking effect of ribulose-1,5-bisphosphate carboxylase oxygenase (RuBisCO) as this protein was identified in almost all fractions including those having an increase in absorbance. Depletion of this protein from crude plant protein extracts is likely to improve protein identification by mass spectrometry, especially for the low abundant proteins. A number of proteins were identified in each fraction and it was difficult to discern which of the proteins was responsible for the differential increase or reduction in absorbance.

Keywords: *Botrytis cinerea*, *Arabidopsis thaliana*, necrotroph, proteome, ProteomeLab PF2D.

INTRODUCTION

Grey mould is one of the major diseases affecting the horticultural industry throughout the world (Staats et al., 2005). It is caused by the necrotrophic fungus *Botrytis cinerea* Per. Fr. (anamorph) and is hosted by more than 200 plant species including grapes, strawberries, raspberries, tomatoes, cucumber, roses, gerbera, onions and other field crops of economic importance (Staats et al., 2005). Besides having a wide host range, *B. cinerea* can infect any part of the plant at any stage of growth although it is more destructive on mature or senescent tissues (Williamson et al., 2007). This pathogen is responsible for pre-harvest as well as massive post-harvest damage, especially among fruits and vegetables (Droby and Lichter, 2004). Post-harvest damage not only decimates the overall crop yield but also results in

*Corresponding author. E-mail: j.mulema@cabi.org. Tel: +254207224450.

Abbreviations: 2D LC, Two-dimensional liquid chromatography; **RuBisCO,** ribulose-1,5-bisphosphate carboxylase oxygenase.

reduced quality of most horticultural products (Williamson et al., 2007). Due to these enormous pre- and post-harvest losses, the pathogen has to be managed and in most cases this has been achieved through the less expensive, but not very effective, biological and cultural control methods (Dik et al., 1999). Chemical control offers the best choice but unfortunately this cannot be used at the time when the produce is ready for consumption since this is the most susceptible stage of the host to this pathogen (Murphy et al., 2000). In addition, chemicals are expensive, and excessive use results in pathogen resistance rendering them less effective and they can be detrimental to the environment (Leroux et al., 2002). Host resistance remains the most cost effective method for managing *B. cinerea* (Elad and Evensen, 1995). However, to achieve this, it is necessary to have a good understanding of the host defence mechanisms against the pathogen.

A number of biochemical and genetic studies have demonstrated defensive responses induced in plants following pathogen invasion. Early events include the influx of calcium ions (Stab and Ebel, 1987; Bach et al., 1993), alkalinisation of the extracellular medium (Felix et al., 1993) and the generation of reactive (active) oxygen species (ROS), especially the hydroxyl radical, super-oxide ion and the dismutation product, H_2O_2 (Levine et al., 1994; Lamb and Dixon, 1997; Tiedemann, 1997). Reactive oxygen species enhance resistance through cross-linking of cell wall proteins rendering the cell wall more resistant to attack by fungal enzymes and also act as secondary messengers in the activation of the hypersensitive response (HR) (Lamb and Dixon, 1997). The HR is a type of programmed cell death but differs from cell death by necrosis because it requires active plant metabolism and depends on activity of the host transcriptional machinery (He et al., 1994; Dangl et al., 1996). The HR appears to function by isolating the pathogen and depriving it of essential nutrients and impeding its spread if it requires living cells as a conduit for movement (Lamb and Dixon, 1997). Although, the HR significantly reduces continued colonization by biotrophic pathogens, it is opportunistically exploited by necrotrophs including *B. cinerea* to promote host cell death (Govrin and Levine, 2000; Schouten et al., 2002; Tenberge et al., 2002). Biosynthesis and accumulation of an array of endogenous signalling compounds especially salicylic acid, ethylene and jasmonic acid has also been reported. These signalling compounds activate signal transduction cascades that eventually result in activation of pathogen-responsive genes. In recent years, the ultimate aim has been to identify pathogen-responsive genes through global transcriptome profiling following host infection with pathogens.

In previous work, oligonucleotide microarrays (Rensink and Buell, 2005) were employed to identify differential gene expression in space (spatial) and time (temporal) in *Arabidopsis thaliana* (thereafter *Arabidopsis*) leaves when infected with *B. cinerea* (Mulema, 2008; Mulema and Denby, 2011). In this study, four-week-old *Arabidopsis* leaves were inoculated with *B. cinerea* and harvested after 12 and 24 hpi for the temporal study, while for the spatial study, *Arabidopsis* leaves of the same age were inoculated with a single drop of *B. cinerea* spore suspension in the middle of the leaf. Using a cock borer of 6 mm in diameter, leaf disks were cut from the edge of the lesion (0 to 6 mm) (proximal tissue) and exactly after the first cut (6 to 12 mm) (distal tissue) after 48 hpi. A multitude of genes induced spatially and temporarily were identified. For the temporal study, some genes were specifically up- and down-regulated at 12 and 24 h, while others were up- and down-regulated at both time points. Similarly, some genes were specifically induced close to the lesion and distal tissue, while others were close to proximal and distal tissue. Clustering of expression profiles resulting from *B. cinerea* and other biotic and abiotic interactions with *Arabidopsis* indicated a large overlap in gene expression profiles (Mulema, 2008; Mulema and Denby, 2011).

The information generated from transcriptome profiling studies gives an insight on events happening at molecular level but is not sufficient to elucidate the functioning of biological systems, especially at the molecular level (Patterson, 2004; Reddy, 2007). These studies only provides information about the abundance of mRNA, which is the only the first step in long sequence of events that lead to the formation of proteins, the main working molecules of cells (Lodish et al., 2004). For instance, a number of post-transcriptional modifications especially addition of a 5' cap, a poly(A) tail and splicing to remove introns take place following mRNA modification. Through alternative splicing, a molecular process common in eukaryotes, a single mRNA may generate dozens of different mRNA isoforms all giving rise to different proteins (Lareau et al., 2004; Stamm et al., 2005; Reddy, 2007). In addition, proteins undergo a number of post-translation modifications following translation either in the form of covalent modifications (such as acetylation, carboxylation, glycosylation, hydroxylation, methylation, nitrosylation, phosphorylation, transamidation and ubiquitination) or proteolytic cleavage at specific amino acid residues (Blom et al., 2004; Gomord and Faye, 2004; Kwon et al., 2006). Due to such modifications, the number of expressed transcripts is not always suggestive of the corresponding translated proteins at either steady state or in response to a stimulus. This supposition is supported by many studies that have shown a poor correlation between the transcribed mRNA and expected translation products (Gygi et al., 1999; Ideker et al., 2001; Kern et al., 2003). The main objective of this study was to determine whether the type of proteins induced in *Arabidopsis* in response to infection with *B. cinerea* correspond to expressed and repressed genes in the microarray experiment.

Principally, protein expression studies whether in cells

or tissues have been carried out using gel-based two-dimensional methods (2-DE) especially two dimension sodium dodecyl sulphate polyacrylamide gel electrophoresis (2D SDS-PAGE) (Klose, 1975; Gorg et al., 1999; Patton, 2002; Peck, 2005). In these methods, proteins are separated based on their isoelectric point (p*I*) in the first dimension and molecular weight (*Mr*) in the second dimension. Identification of proteins is achieved by in-gel proteolytic digestion coupled with MALD-MS peptide mass fingerprinting. Consequently, resolution of more than 1000 protein spots is possible on a single gel especially where the protein isoelectric points and molecular weights can be estimated. Level of expression can be obtained by measuring the optical density of each spot. For this reason, 2-DE methods are important in protein expression studies especially when differences in protein isoelectric points, molecular weights or expression levels can be visualized. However, these methods present fundamental problems and limitations. They are very laborious, time consuming, and are not particularly good at resolving low abundance, low molecular weight, very large, hydrophobic or membrane proteins and those with extreme p*I* values (Hamler et al., 2004; Peck, 2005; Yan and Chen, 2005). Reproducibility of protein expression patterns across laboratories is very difficult, as these patterns are highly dependent on experimental conditions and procedures (Viswanathan et al., 2006). In addition, silver staining, the most common staining technique used for protein spot visualization with these methods, is protein dependent and suffers from a poor dynamic range (Westermeier and Marouga, 2005; Grove et al., 2009). Non-gel based methods especially the two dimension liquid chromatography (2-D LC) methods mitigate all limitations experienced with 2-DE methods. In these methods, proteins are separated (eluted) based on pH (chromatofocusing, CF) in the first dimension and hydrophobicity in the second dimension (Mann et al., 2001; Zhu et al., 2003). A 2-D LC method, ProteomeLab™ PF2D (Beckman Coulter, Inc. USA) was used in this study. This method has been widely used in protein expression studies (Chang et al., 2007).

MATERIALS AND METHODS

Plant growth and infection

Arabidopsis plants of the ecotype Columbia-0 were grown for four weeks in a mixture of soil composed of peat plugs (Jiffy Products, International AS, Norway) and vermiculite in a 1:1 ratio. Using the detached leaf method (Mulema, 2008), *Arabidopsis* leaves were inoculated (8 to 10 drops of 10 µl spore suspension placed on top of the leaf) with the pepper isolate of *B. cinerea* (Denby et al., 2004). The spores were placed in half strength grape juice (Ceres Fruit Juices (Pty) Ltd, South Africa) and the concentration was adjusted to 500,000 spore/ml. Control leaves were treated with half strength grape juice containing no spores. Inoculated and mock-treated leaves were harvested at 6, 12 and 24 h post inoculation (hpi). This experiment was biologically replicated (three) and in all cases, inoculations were carried out at the same time of the day on non-bolting plants of the same age (four weeks).

Protein sample preparation

One gram of mock-treated and inoculated *Arabidopsis* leaf tissue was ground in liquid nitrogen to a fine powder and 2 ml of lysis denaturing buffer {5 M urea, 2 M thiourea, 10% (v/v) glycerol, 50 mM Tris-HCl (pH 7.8 to 8.2, between 10 to 25°C), 2% (w/v) *n*-octylglucoside (octyl α-D-glucopyranoside), 2.5% (w/v) N-decyl-N,N-dimethyl-3-ammonio-1-propane sulfonate (SB3-10), 5 mM Tris (2-carboxyethyl) phosphine hydrochloride (TCEP) and 1 mM protease inhibitor cocktail (Sigma-Aldrich, Gillingham, Dorset, UK)} was added. The mixture was vortexed for 1 min, sonicated for 5 min and finally centrifuged at 9,447 x*g* for 60 min. The supernatant was stored at -20°C until use. Prior to injection into the chromatofocusing (CF) column, protein extract was desalted and equilibrated to the column environment using the PD-10 desalting column (Amersham Biosciences, United Kingdom). Column equilibration was performed with 25 ml of CF start buffer (Beckman Coulter Inc. CA USA) and 2.5 ml of the protein extract was loaded. The column was washed with CF start buffer and the first 3.5 ml fraction was collected. Protein concentration of the eluent was determined using the Bradford assay (Bradford, 1976). An equivalent of 5 mg of protein was diluted with start buffer to bring the volume for each sample to 7 ml. Only one repetition of this study was subjected to downstream experiments.

First dimension: Chromatofocusing

CF was performed on an HPCF-1D column (Beckman Coulter Inc. CA USA). Before use, the start and eluent buffers were calibrated by sonication for 5 min followed by pH adjustment to 8.5 and 4.0, respectively using either a saturated solution of 50 mg/ml iminodiacetic acid or 1 M NH_4OH. The CF column was equilibrated with calibrated start buffer to an initial pH of 8.5 for 210 min at a flow rate of 0.2 ml/min. The sample (7 ml) was manually injected onto the CF column for first dimension separation. Start buffer was pumped through the column for the first 35 min to elute proteins with p*I* values above 8.5. After 35 min, a pH gradient from 8.5 to 4.0 was started by introduction of the eluent buffer (pH 4.0) and this continued up to 130 min. After the pH gradient, the most acidic proteins were recovered by washing the column with 1 M NaCl for 25 min followed by a final wash in water for 45 min. Protein fractions were eluted based on their p*I*, measured for absorbance at 280 nm, and collected in a 96 deep-well plate by a fraction collector according to predetermined pH decrements of 0.3 pH units during the pH gradient, or in 1.5 ml volumes before and after the pH gradient.

Second-dimension: High performance reversed-phase chromatography

High performance reverse-phase chromatography was carried out on an HPRP 2D column (Beckman Coulter, Inc. CA USA), which was pre-equilibrated with 0.1% (v/v) trifluoroacetic acid (TFA) in water. The mobile phase consisted of 0.1% (v/v) TFA in water (A) and 0.08% (v/v) TFA in acetonitrile (B). Separation was performed at 0.75 ml/min with an increasing gradient of B. During the first 2 min, 100% of A was pumped into the column; in the next 35 min, the gradient was created in the column by switching the flow from 0 to 100% B; this was followed by 100% B for 4 min and 100% A for 9 min. An aliquot of 500 µl of each of the selected first-dimension fractions was run and fractions were collected in a 96-well plate by an automated fraction collector at intervals of 15 s between 4 and 24 min. Collected second-dimension fractions were stored at -80°C for subsequent mass spectrometry analysis.

Data analysis

Multiple chromatography traces from the second dimension separation were converted into 2D protein expression maps by importation into the ProteoVue software program (Beckman Coulter, Inc. CA USA). Differential protein expression of control and treatment samples was determined by comparing two ProteoVue 2D protein expression maps with the assistance of the DeltaVue software package (Beckman Coulter, Inc. CA USA). The analysis was based on comparing the peak height of proteins and peptides that elute in the same pH fraction in the first dimension and at the same time in the second dimension.

Mass spectrometry and protein identification

An aliquot of 175 µl of each selected fraction was completely evaporated under vacuum. To each fraction, 10 µl of 100 mM NH_4HCO_3 and 15 µl of 10 mM DTT were added and incubated for 30 min. Alkylation was achieved by incubating with 15 µl of 55 mM iodoacetamide for 20 min. The mixture was digested with 12.5 µl Trypsin (6 ng/µl) and incubated at 37°C for 3 h. The samples were resuspended in 20 µl of 0.1% formic acid and transferred to a CapLC system (Waters Corporation). An aliquot of 6.4 µl was mixed with 13.6 µl of 0.1% formic acid and loaded onto a 0.5 cm LC Packings C18 5 µm, 100 Å, 300 µm i.d. pre-column cartridge. Flushing the column with 0.1% formic acid desalted the bound peptides before a linear gradient of solvent B (0.1% formic acid in acetonitrile) at a flow rate of approximately 200 nl/min eluted the peptides for further resolution on a 15 cm LC Packings C18 5 µm, 5 Å, 75 µm i.d. PepMap analytical column. The eluted peptides were analyzed on a Micromass Q-Tof Global Ultima (Waters Corporation) mass spectrometer fitted with a nano-LC sprayer with an applied capillary voltage of 3.5 kV. The instrument was calibrated against a collisionally induced dissociation (CID) spectrum of the doubly charged precursor ion of [Glu^1]-fibrinopeptide B (GFP) and operated in data dependent acquisition (DDA) mode over the mass/charge (m/z) range of 50 to 2000. During the DDA analysis, both MS and tandem mass spectrometry (CID) was performed on the most intense peptides as they eluted from the column. The uninterpreted MS/MS data were processed (smoothed, background subtracted, centered and deisotoped) using the Micromass ProteinLynx Global Server v2.3 which then searched the MS/MS spectra against an appropriate database using the Micromass Global Server 2.2 search engine. Search parameters specified were 100 ppm tolerance against the database-generated theoretical peptide ion masses and a minimum of one matched peptide. A list of the twenty highest scoring entries was produced and each suggested protein identification was confirmed or rejected by a comparison of the theoretical sequence with observed MS/MS data. When the database search was unsuccessful, the MS/MS spectra were interpreted in order to obtain amino acid sequence tags. Spectra were interpreted automatically using the Peaks Studio 4.5 software package (Disinformation Solutions Inc.) then manually verified and/or improved by manual intervention and probabilistic peptide sequences suggested.

Functional categorization

A list of genes encoding proteins identified in fractions that displayed an increase (up-regulated) or reduction (down-regulated) in absorbance were uploaded into the web-based application FatiGO (http://fatigo.bioinfo.cipf.es) (Al-Shahrour et al., 2004) to extract relevant gene ontology terms. These lists were separately compared with the whole genome list from which those genes had been removed. The gene ontology level 3 was selected because this constitutes a good compromise between information quality and number of genes annotated.

RESULTS

The 2D LC system ProteomeLab PF2D was used to separate proteins based on their p*I* and hydrophobicity in the first and second dimensions, respectively. The first dimension resolved total protein into 36 fractions for each time point (6, 12 and 24 h post inoculation, hpi). Each of the 36 fractions was further resolved into 54 fractions in the second dimension; hence, proteins from leaves at each time point were separated into 1,836 fractions. Chromatographic absorbance intensities from 12 p*I* fractions after second dimension fractionation are shown for one sample in Figure 1. Despite the presence of one strong band in all fractions, additional bands varying between fractions are clearly visible. Differential expression of proteins from corresponding fractions of 24 h mock and infected samples is shown in Figure 2. Several bands (proteins) that increased or are only detectable in the infected leaf sample as compared to the mock-inoculated are clearly visible. All 1^t dimension fractions contained differentially expressed bands of protein demonstrating expression of large number of proteins with a wide range of p*I* in response to infection. Comparing chromatogram peaks corresponding to proteins of the same p*I* and hydrophobicity in the two samples allows quantification of the differences between mock and infected proteomes. Peaks that displayed differential expression between the mock and treated samples were selected from fir and fine adjustments were made on the intensities of the selected peaks using the baseline correction function to give a more accurate expression level difference.

Fractions containing peaks that displayed differential expression of more than 2-fold increase or reduction in absorbance between the mock and infected samples were selected for protein identification. Because these fractions were selected based on absorbance change of the whole fraction, the number of the proteins that are changed in absorbance, which of the proteins changed and whether changes in one protein are masking changes (example down-regulation) of other proteins, are not known. Based on the 2-fold increase or reduction in absorbance criterion, 10, 92 and 66 fractions were selected at 6, 12 and 24 hpi, respectively (data not shown). Each of these fraction contains multiple proteins but changes in total absorbance of the corresponding fractions from mock and inoculated samples indicate differential expression of at least one protein. The number of proteins identified in the selected fractions ranged from 1 to 10 with some of the proteins identified in more than one fraction. In fractions showing an increase in absorbance of proteins at 6 hpi, only RuBisCO activase (At2g39730) was identified. However, this protein was also identified in down-regulated fractions at 12 and 24 hpi (Table 2). Five and eight proteins were identified in fractions that

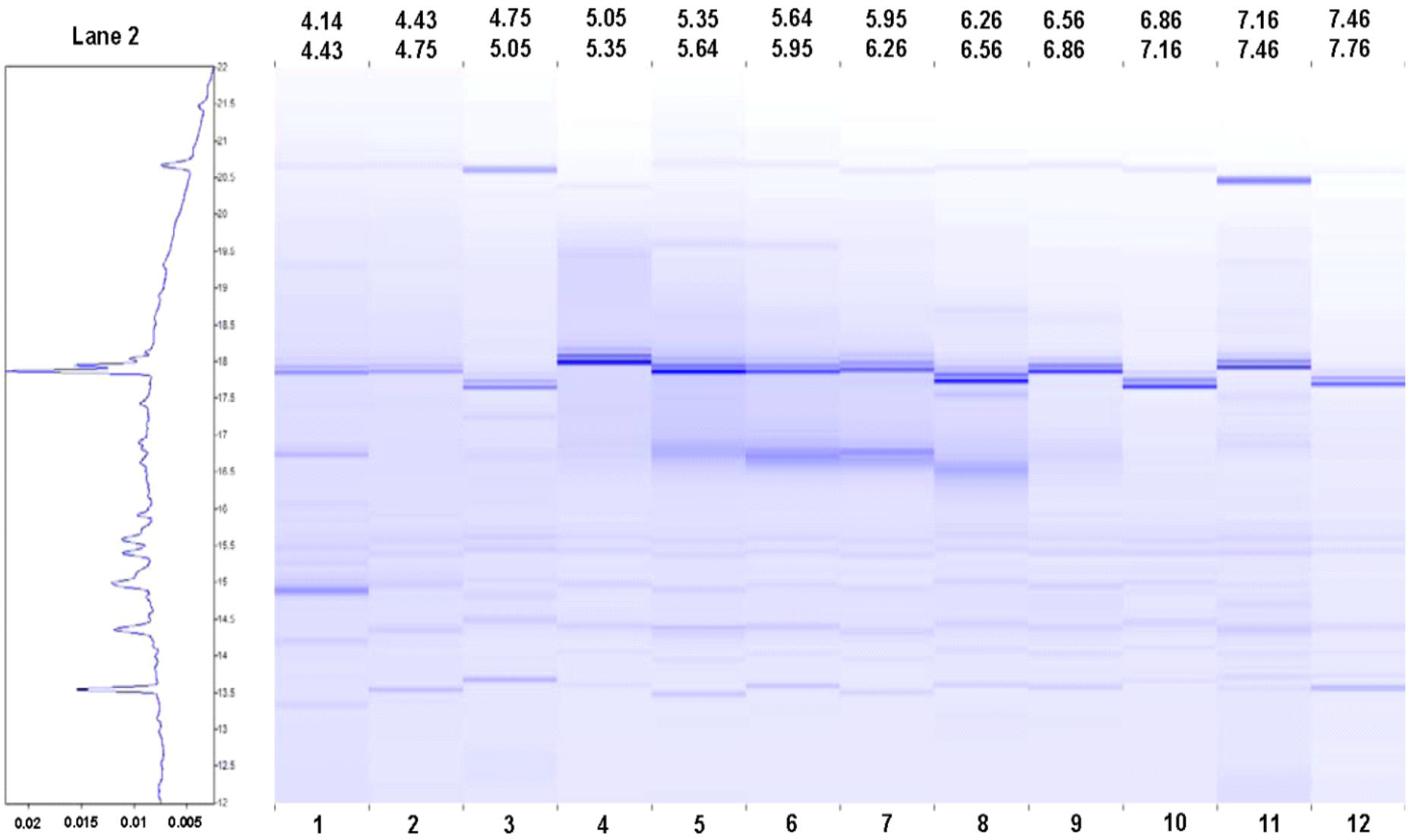

Figure 1. The two-dimensional map of absorbance at 280 nm obtained for crude protein extracted from infected Arabidopsis leaf tissue (24 hpi) as viewed with ProteoVue. Each lane represents the absorbance intensity of the 2nd dimension separation of each fraction collected in during 1st dimension separation. Only 12 of the 34 1st dimension fractions are shown. At the top of each lane is the starting and ending pH of each 1st dimension fraction. To the left is the chromatogram for a given fraction, which is located with the cursor in the software. A common band, which is possibly RuBisCO, was fractionated after about 18 min in all fractions

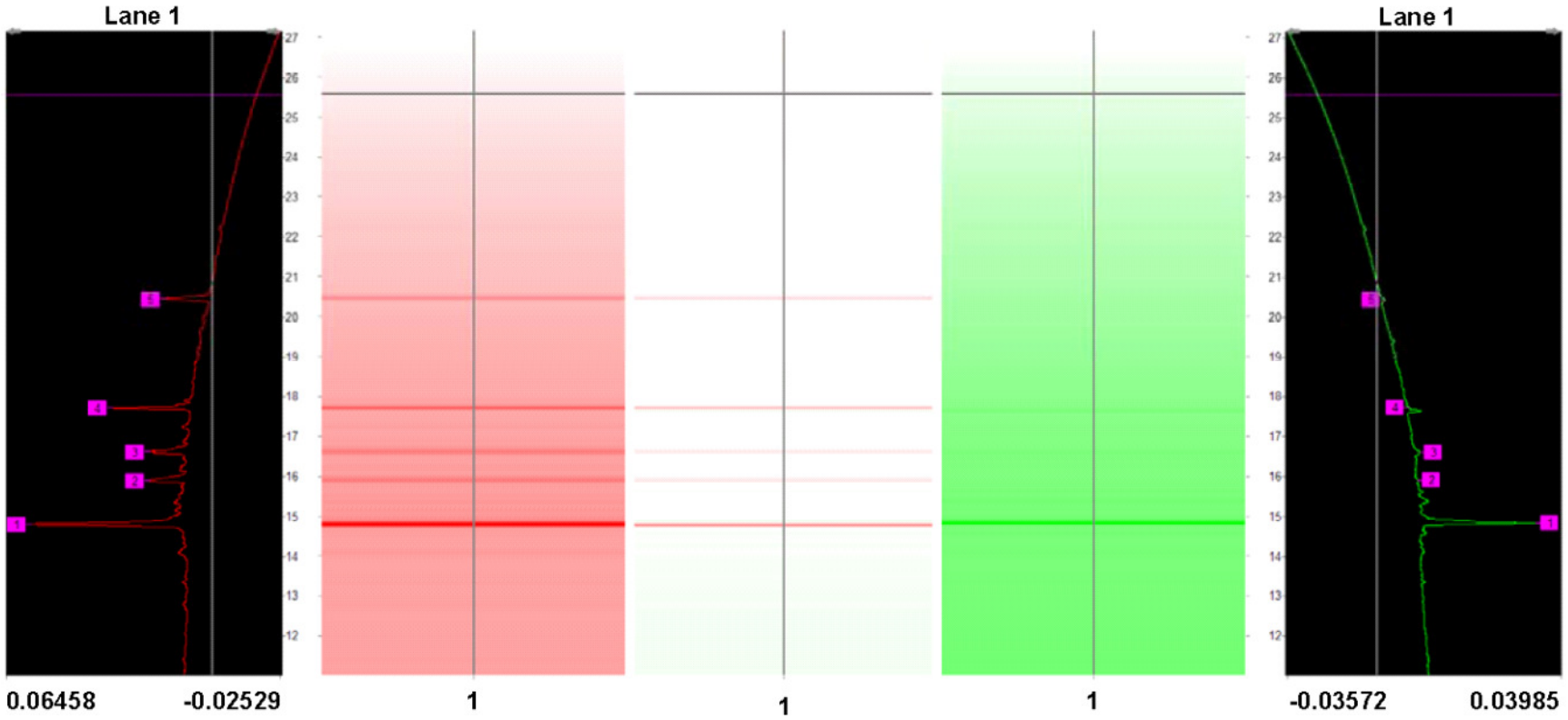

Figure 2. Differential expression of proteins from the second dimension fractionation of Arabidopsis leaf tissue 24 h after infection with *B. cinerea* (left, red) and mock inoculation (right, green) as viewed in DeltaVue. Each lane (example lane 1 shown above) represents the absorbance of the protein fraction at 280 nm while the UV chromatograms for the 2nd dimension separation for corresponding lane (lane 1) are shown on the outside of the map. The centre portion between the maps shows the qualitative and quantitative differences between samples where the intensity of the colour represents the abundance of the proteins associated with the peaks. Therefore, the colour that is displayed corresponds to the sample with the protein in a greater amount. In this case, the infected sample has more protein than the mock treated sample.

displayed an increase in absorbance in infected leaves and 12 and 24 hpi, respectively (Table 1). Three of the proteins (At1g02930, At2g02930 and At4g02520) were also identified at both time points. A much larger number of proteins were identified in fractions displaying a reduction in absorbance in infected as compared to mock samples (Table 2). At 6, 12 and 24 hpi 13, 72 and 55 proteins were identified, respectively. Several proteins were identified at multiple time points; 6, 3 and 24 proteins were common between 6 and 12 h, 6 and 24 h and 12 and 24 h, respectively. Only two proteins, At3g50820 (oxygen-evolving complex) and At2g39730 (RuBisCO activase) were identified in fractions at all three-time points. Specific proteins were identified in fractions that differed in absorbance between infected and mock-inoculated leaves. However, as multiple proteins are likely to be present in a single fraction, it is not possible to unequivocally pinpoint the differentially expressed protein(s). Hence, these

Table 1. Proteins present in fractions showing an increase in absorbance after 12 and 24 hpi in *B. cinerea* infected Arabidopsis leaf tissue as compared to mock.

Accession	Locus	p*I*	MW (Da)	Coverage (%)	Description
12 hpi					
IPI00548409	At1g02930	5.8	23471	4.8	Glutathione S-transferase
IPI00544607	At1g20620	6.3	48867	5.9	Catalase 1
IPI00532945	At2g02930	6.5	24106	3.8	Glutathione S-transferase
IPI00535149	At4g02520	5.9	24114	14.6	Glutathione S-transferase
IPI00656658	At1g07890	5.9	27502	18.5	Ascorbate peroxidase
24 hpi					
IPI00607519	At1g02920	6.1	23583	11	Glutathione S-transferase
IPI00548409	At1g02930	5.8	23471	11.1	Glutathione S-transferase
IPI00532945	At2g02930	6.5	24106	13.2	Glutathione S-transferase
IPI00529373	At3g04720	7.9	22921	3.8	PR4 (Hevein-like protein)
IPI00535348	At3g15356	9.5	29593	4	Lectin like protein
IPI00522050	At3g49120	7.6	38807	7.1	Peroxidase
IPI00535149	At4g02520	5.9	24114	22.2	Glutathione S-transferase
IPI00517541	At5g40370	6.7	11748	12.6	Glutaredoxin

Columns show accession number (EBI database), gene locus, theoretical p*I* and molecular weight (MW) in daltons (Da), percentage coverage and protein description. MW and p*I* were calculated from the sequence of the protein in the EBI database. The percentage coverage represents the amount of protein sequence covered by the matched peptides.

Table 2. Proteins present in fractions showing a decrease in absorbance after 12 and 24 hpi in *B. cinerea* infected Arabidopsis leaf tissue as compared to mock.

Accession	Locus	p*I*	MW (Da)	Coverage (%)	Description
6 hpi					
IPI00520638	At1g32470	5.1	17886	9.6	Glycine cleavage system H protein
IPI00521992	At1g36940	10.3	20242	3.9	Unknown protein
IPI00541680	At1g42970	6.3	47630	2.2	Glyceraldehyde-3-phosphate dehydrogenase
IPI00541637	At1g55040	6.6	94805	1.3	Zinc finger (Ran-binding) family protein
IPI00534914	At1g79330	6.2	44818	2.9	Caspase family protein
IPI00527972	At2g36880	5.8	42471	3.9	Methionine Adenosyltransferase
IPI00520309	At2g39730	7.6	48469	22.9	RUBISCO activase
IPI00544162	At2g45590	8.8	75506	2.8	Protein kinase family protein
IPI00522872	At3g26740	4.6	15304	12.1	Light responsive protein-related
IPI00519769	At3g50820	5.9	34998	18.7	Oxygen-evolving enhancer protein
IPI00534852	At5g35630	6.4	47381	1.9	Chloroplastic glutamine synthetase
IPI00656706	At5g38410	8.2	19383	4.6	RuBisCO small subunit 3B
IPI00545883	At5g66570	5.6	35120	33.7	Oxygen-evolving enhancer protein
12 hpi					
IPI00537832	At1g03130	9.8	22293	4.9	Photosystem I reaction center
IPI00531916	At1g03600	9.9	18823	5.7	Photosystem II family protein
IPI00535457	At1g03680	9.1	19652	14	Thioredoxin
IPI00518864	At1g04410	6.1	35548	9.3	Malate dehydrogenase
IPI00540742	At1g06680	5.9	28078	3.8	Oxygen-evolving enhancer protein
IPI00846137	At1g07930	9.3	41348	3	Elongation factor 1-alpha
IPI00538278	At1g11860	8.6	44416	3.9	Aminomethyltransferase
IPI00846619	At1g12900	6.2	34311	7.6	Glyceraldehyde 3-phosphate dehydrogenase
IPI00846497	At1g13440	6.8	33885	14.2	Glyceraldehyde 3-phosphate dehydrogenase
IPI00524841	At1g13930	4.8	16154	16.1	Nodulin-related

Table 2. Continue

IPI00846186	At1g19570	5.6	23440	3.8	Dehydroascorbate reductase
IPI00520177	At1g20340	5.1	16973	14.4	Plastocyanin
IPI00846719	At1g26630	5.7	15093	7.2	Eukaryotic translation initiation factor
IPI00525222	At1g30380	10.5	13198	6.9	Photosystem I reaction center
IPI00535877	At1g31330	9.6	24158	5	Photosystem I reaction center
IPI00520638	At1g32470	5.1	17885	9.6	Glycine cleavage system H protein
IPI00518517	At1g45249	9.4	43101	2.5	ABA responsive elements-binding factor
IPI00539020	At1g67090	7.6	20203	46.7	RuBisCO
IPI00548733	At1g79850	10.6	16272	6.7	30s Ribosomal protein
IPI00520709	At1g80240	8.5	40200	2.2	Expressed protein
IPI00533812	At2g03440	7.5	19689	5.9	Nodulin-related
IPI00657461	At2g21330	6.3	33302	7.4	Fructose-bisphosphate aldolase
IPI00529898	At2g21870	9	25144	5	ATP Synthase
IPI00528969	At2g24260	6.4	36499	2.6	Basic helix-loop-helix family protein
IPI00536157	At2g35370	5.2	17935	9.7	Glycine cleavage system H protein
IPI00526310	At2g36530	5.5	47689	4.7	Enolase
IPI00527972	At2g36880	5.8	42470	3.8	Methionine adenosyltransferase
IPI00540246	At2g37220	5.1	30699	3.1	Putative ribonucleoprotein
IPI00527785	At2g38540	9.3	11747	15.3	Non-specic lipid-transfer protein
IPI00520309	At2g39730	7.6	48469	15.4	RuBisCO activase
IPI00519410	At3g13470	5.6	63302	6	Chaperonin
IPI00846962	At3g15020	9.5	33113	5.1	Malate dehydrogenase
IPI00529886	At3g15360	9.6	21159	10.9	Thioredoxin
IPI00536966	At3g17390	5.5	42768	4.8	S-adenosylmethionine synthase
IPI00518644	At3g22890	6.3	51427	2.2	ATP Sulfurylase
IPI00537303	At3g26650	7.6	42463	2	Glyceraldehyde 3-phosphate dehydrogenase
IPI00519769	At3g50820	5.9	34998	25.1	Oxygen-evolving enhancer protein
IPI00523226	At3g52150	6.8	59745	2	Uncharacterized protein
IPI00533612	At3g52960	9.1	24669	4.7	Peroxiredoxin
IPI00525581	At3g60210	7.7	15131	6.5	Chloroplast chaperonin
IPI00517879	At3g62030	8.8	28190	3.5	Peptidyl-prolyl cis-trans isomerase
IPI00535044	At3g62410	4.8	14157	9.9	CP12 domain-containing protein
IPI00516646	At3g63140	8.5	43903	2.5	Uncharacterized protein
IPI00545948	At3g63190	9.5	30403	3.6	Ribosome recycling factor
IPI00521950	At4g01900	9.2	21262	5.6	Glutamine synthetase
IPI00530995	At4g03280	8.6	22518	6.7	Isoform 2 of Cytochrome B6-F complex
IPI00525302	At4g04640	8.1	40886	3.5	ATP synthase gamma chain
IPI00548616	At4g05180	9.7	24628	19.1	Oxygen-evolving enhancer protein
IPI00656759	At4g08870	6.6	29295	3.8	Arginase
IPI00521214	At4g09320	8.4	18802	5.3	Nucleoside diphosphate kinase
IPI00535216	At4g10340	6	30138	3.6	Chlorophyll A-B binding protein
IPI00530817	At4g18480	6.1	46241	2.4	Magnesium-chelatase subunit
IPI00532377	At4g20260	5	24568	5.8	DREPP plasma membrane polypeptide
IPI00532582	At4g21280	9.6	23781	9.9	Oxygen-evolving enhancer protein
IPI00531287	At4g24280	5.1	76461	1.3	Chloroplast heat shock protein
IPI00546869	At4g27520	9.4	35042	2.6	Early nodulin-like protein
IPI00532440	At4g28750	9.9	14958	9.1	Photosystem I reaction center
IPI00525727	At4g37930	8.1	57364	8.9	Serine hydroxymethyltransferase
IPI00541448	At4g38970	6.8	42915	8	Fructose-bisphosphate Aldolase
IPI00519631	At5g03850	10.8	7366	18.8	40S ribosomal protein
IPI00657400	At5g09660	7.6	34953	3.3	NAD-malate dehydrogenase
IPI00523587	At5g14740	5.4	28326	6.6	Carbonic anhydrase
IPI00537160	At5g15970	9.1	6547	37.9	Stress-induced protein kinase

Table 2. Continue

IPI00521944	At5g26780	8.8	57305	1.7	Serine hydroxymethyltransferase 2
IPI00534852	At5g35630	6.4	47381	7.4	Glutamine synthetase
IPI00656706	At5g38410	8.2	19383	16.7	RuBisCO
IPI00523477	At5g38420	7.6	20337	33.7	RuBisCO
IPI00521186	At5g38430	7.8	20273	24.9	RuBisCO
IPI00518961	At5g49910	5.2	76949	1.8	Heat shock protein
IPI00523656	At5g55220	5.3	61695	2.4	Trigger factor type chaperone
IPI00531316	At5g63400	6.9	26915	6.1	Adenylate kinase
IPI00547610	At5g64040	9.1	18417	29.8	Photosystem I reaction center
24 hpi					
IPI00531916	At1g03600	9.9	18823	7.5	Photosystem II family protein
IPI00518864	At1g04410	6.1	35548	2.4	Malate dehydrogenase
IPI00846137	At1g07930	9.3	41347	3	Elongation factor 1
IPI00846497	At1g13440	6.8	33884	4.5	Glyceraldehyde 3-phosphate dehydrogenase
IPI00524194	At1g15820	6.8	27505	3.9	Light harvesting complex PSII
IPI00520177	At1g20340	5.1	16973	14.4	Plastocynin
IPI00543566	At1g53240	8.5	35781	7.3	Malate dehydrogenase
IPI00533812	At2g03440	7.5	19688	5.9	Nodulin-related
IPI00541933	At2g21660	5.4	15539	13.2	Glycine-rich RNA-binding protein
IPI00525237	At2g28000	5.1	62033	3.4	Chaperonin-60
IPI00527785	At2g38540	9.3	11746	8.5	Nonspecific lipid transfer protein 1
IPI00520309	At2g39730	7.6	48469	2.5	RuBisCO activase
IPI00544162	At2g45590	8.8	75506	2.8	Protein Kinase famlity protein
IPI00527415	At3g01390	5.8	12389	20.9	Vacuolar ATP synthase
IPI00657469	At3g01500	5.3	28180	18.9	Carbonic anhydrase
IPI00521134	At3g06050	9	21432	5.5	Peroxiredoxin-2F
IPI00846962	At3g15020	9.5	33112	3.8	Malate dehydrogenase
IPI00522229	At3g16140	10	15207	7.6	Photosystem I reaction center
IPI00529853	At3g20390	9.2	27782	23.9	Translational inhibitor protein
IPI00548978	At3g26060	9.5	23663	7.4	Peroxiredoxin Q
IPI00525750	At3g47070	9.7	10523	26	Thylakoid soluble phosphoprotein
IPI00519769	At3g50820	5.9	34997	3.6	Oxygen-evolving enhancer protein
IPI00523226	At3g52150	6.8	59744	2	RNA-binding family protein
IPI00532442	At3g53430	9.1	17958	9	60S ribosomal protein
IPI00535044	At3g62410	4.8	14157	9.9	CP12 domain-containing protein
IPI00545948	At3g63190	9.5	30403	3.6	Ribosome recycling factor
IPI00529234	At4g01150	9.2	17686	6.1	Unkown protein
IPI00530995	At4g03280	8.6	22518	5.7	Rieske FeS center of cytochrome b6f complex
IPI00521214	At4g09320	8.4	18801	5.3	Nucleoside diphosphate kinase
IPI00528276	At4g09650	9.1	25652	4.3	ATP synthase
IPI00535216	At4g10340	6.0	30137	3.6	Chlorophyll A-B binding protein
IPI00533660	At4g10790	4.9	52770	2.1	UBX domain-containing protein
IPI00519731	At4g14880	7.0	52980	2.3	O-acetylserine(thiol)lyase
IPI00846603	At4g18360	7.7	34382	3.2	(S)-2-hydroxy-acid oxidase
IPI00520474	At4g20360	5.8	51597	2.3	RAB GTPASE homolog E1B
IPI00532582	At4g21280	9.6	23780	30.5	Photosystem II Subunit QA
IPI00544207	At4g21850	7.6	13512	7.4	Methionine sulfoxide reductase
IPI00531287	At4g24280	5.1	76461	3.1	Chloroplast heat shock protein
IPI00546869	At4g27520	9.4	35042	2.6	Plastocyanin-like domain-containing protein
IPI00532440	At4g28750	9.9	14957	9.1	PSA E1 Knockout
IPI00534382	At4g34870	8.9	18366	8.1	Rotamase cyclophilin

Table 2. Continue

IPI00525727	At4g37930	8.1	57364	2.3	Serine transhydroxymethyltransferase
IPI00516234	At5g08690	6.2	59676	4.1	ATP synthase
IPI00522652	At5g13710	5.9	38244	2.4	Cycloartenol-C-24-methyltransferase
IPI00524759	At5g20630	6.3	21822	5.2	Germin-like protein
IPI00521186	At5g38430	7.8	20273	12.2	RuBisCO
IPI00549113	At5g38570	6.8	47719	1.7	F-box family protein
IPI00542973	At5g40770	7.0	30381	4	Prohibitin
IPI00532635	At5g45680	9.0	22025	8.7	FK506-binding protein
IPI00518961	At5g49910	5.2	76949	3.1	Heat shock protein
IPI00527963	At5g56210	4.9	56479	2.6	WPP-domain Interacting protein
IPI00519434	At5g57950	5.2	30114	2.9	26S proteasome regulatory subunit
IPI00542817	At5g59880	5.0	14115	9.7	Actin depolymerizing factor
IPI00657184	At5g63400	6.3	20805	7.4	Adenylate kinase
IPI00525776	Atcg00480	5.4	53900	11	ATP synthase

Columns show accession number (EBI database), gene locus, theoretical p*I* and molecular weight (MW) in daltons (Da), percentage coverage and protein description. MW and p*I* were calculated from the sequence of the protein in the EBI database. The percentage coverage represents the amount of protein sequence covered by the matched peptides.

results were validated in various ways; first, all identified proteins were subjected to functional categorization based on the biological process gene ontology (Ashburner et al., 2000) to look for over-represented functional categories. Identification of several proteins involved in the same biological process support the likelihood that this process is involved in defence and the proteins truly differentially expressed. Among the over-represented categories for proteins identified in fractions with increased absorbance in infected samples as compared to mock were responsive to chemical stimulus and catabolic process at 12 hpi and secondary metabolic process at 24 hpi (Table 3). The major categories for the proteins identified from fractions that displayed a reduction in absorbance in infected leaves were photosynthesis and carbon utilization common to 12 and 24 hpi and response to abiotic stimulus and nitrogen compound metabolic process at 12 hpi (Table 3). Second, the genes encoding proteins identified in this study were either up-regulated or down-regulated in the gene expression profiling study (Mulema, 2008; Mulema and Denby, 2011) and lastly, the expression profiles of one of these genes (At3g04720) was also confirmed using quantitative polymerase chain reaction (real-time PCR) (Mulema, 2008; Mulema and Denby, 2011). Also, raw data (GenePix results (GPR) files) resulting from the gene expression study has been deposited at National Center for Biotechnology Information (NCBI) under Gene Expression Omnibus; accession numbers GSE24444 (Spatial microarray experiment) and GSE24445 (Temporal microarray experiment).

DISCUSSION

The main objective of this study was to determine if genes observed to increase or decrease in expression in the microarray experiment could correlate with proteins expressed following the same inoculation pattern. In this study, *Arabidopsis* leaves were infected with *B. cinerea* and harvested after 6, 12 and 24 hpi. Crude protein extractions were obtained from leaf tissue harvested at the indicated time points. Proteins in the extractions were separated in the first dimension based on p*I* and the second dimension based on hydrophobicity using a 2D LC system, ProteomeLab PF2D. Proteins were only identified in fractions that displayed differential expression of more than 2-fold increase or reduction in absorbance between mock-treated as compared to inoculated samples. Given that selection was based on absorbance change of the whole fraction, it was not possible to determine how many of the proteins were changed in absorbance, which of the proteins were changed and if changes in some proteins masked changes in other proteins. Also, Proteomelab PF2D did not identify many changes in absorbance of fractions as many proteins in the fractions as expected. However, several of the proteins identified in fractions that displayed either increase or decrease in absorbance corresponded to genes up- and down-regulated in the gene expression profiling study (Mulema, 2008; Mulema and Denby, 2011).

There were no proteins identified in fractions that displayed an increase in absorbance at 6 hpi. In addition, very few proteins were indentified in similar fractions at 12 and 24 hpi. This lack of identification of pathogen-derived proteins could be partly attributed to low concentration in the fractions, which could not have permitted detection, or due to the masking effect of high abundant proteins, especially RuBisCO (Atg538439) and RuBisCO activase (At2g39730). Although, this inoculation method

Table 3. Functional categorization of genes encoding proteins identified in fractions that displayed an increase (up-regulated) and decrease (down-regulated) in absorbance based on biological process; all genes (responsive) encoding identified proteins were compared with the entire (whole) genome to identify broad functional categories based on the high level terms in gene ontology (GO) hierarchy. Level three of the GO was considered and only over-represented functional categories are shown. The P-value represents the significance of the overrepresentation.

Entity	Responsive genes		Whole genome		P-values
	Number	Percentage	Number	Percentage	
Up-regulated proteins					
12 hpi					
Response to chemical stimulus	5	100	939	8.4	1.72×10^{-03}
Catabolic process	4	80	473	4.2	4.40×10^{-03}
24 hpi					
Secondary metabolic process	5	57.1	280	2.5	5.46×10^{-03}
Down-regulated proteins					
12 hpi					
Photosynthesis	3	30	76	0.7	3.43×10^{-10}
Carbon utilization	7	20	13	0.1	4.06×10^{-10}
Response to abiotic stimulus	14	24.1	651	5.8	6.13×10^{-04}
Nitrogen compound metabolic process	10	17.2	325	2.9	8.11×10^{-04}
24 hpi					
Photosynthesis	11	8.4	43	0.4	3.38×10^{-27}
Carbon utilization	12	2.8	3	0	3.21×10^{-12}

was successful in identifying differentially expressed mRNA, identification of differentially expressed proteins may require more directly infected material, which could be obtained through spray inoculation. The proteins identified in fractions that displayed an increase in absorbance have been shown to have a major role in host pathogen interactions. For instance, PR4, catalase 1, glutathione S-transferases (GSTs) and lectins have all been shown to be essential especially in interactions involving necrotrophs (Govrin and Levine, 2000; Sharon and Lis, 2004). Catalase 1 and GSTs are known to protect host cells against active oxygen species (AOS). For instance, catalase 1 mediates the breakdown of hydrogen peroxide by converting it into molecular oxygen and water (Willekens et al., 1997), while GSTs are involved in the biotransformation and detoxification of AOS and many other xenobiotic substances (Marrs, 1996; Coleman et al., 1997). *B. cinerea* is known to produce AOS and a number of pathogenicity factors especially nonhost specific toxins (such as botrydial and oxalic acid) (Deighton et al., 2001; Han et al., 2007). The involvement of proteins in an antioxidant system composed of an array of AOS scavenging enzymes, clearly demonstrating the importance of the infection strategy deployed by *B. cinerea* (Kamoun et al., 1992; Michelmore, 2003; Peleman and van der Voort, 2003). All these proteins belonged to the over-represented functional categories of response to chemical stimulus, catabolic process and secondary metabolic process which correlates with the observations made in the gene expression study (Mulema, 2008; Mulema and Denby, 2011).

The majority of the proteins in this study were identified in fractions that displayed a decrease in absorbance. Although, it is hard to explain why most of the proteins identified in this study were from such fractions, down-regulation is also a known defence response by the host to pathogen invasion (Mulema and Denby, 2011). As expected, most of these proteins are encoded by genes that were identified in the gene expression profiling study except for a few. This underlines the importance of gene expression studies in generating insights of events taking place at the molecular level. Some of the down-regulated genes were shown to be involved in the photosynthetic pathway; this was confirmed by the over-representation of this category. A similar scenario was observed in the gene expression profiling study (Mulema and Denby, 2011). Other gene and protein expression studies have also reported with down-regulation of this pathway in response to both host and nonhost pathogen infection (Chou et al., 2000; Zimmerli et al., 2004). This indicates that this is a response to infection by all groups of pathogens although the magnitude of gene or protein regulation may vary depending on the attacking pathogen. However, the main question is why this phenomenon? This could be because the plant needs to save energy by suppressing a high-energy intensive process in

photosynthesis. This energy could then be available for executing other defence options that may be deployed. However, the plant turns to energy reserves in form of carbohydrates to generate the required energy. Many studies have considered this line of action; for instance Chou et al. (2000) attributed down-regulation of the photosynthetic pathway to elevated levels of soluble carbohydrates as a result of increased invertase activity. In other studies, sugars were shown to down-regulate the expression of RuBisCO and genes involved in photosynthesis (Jang and Sheen, 1994; Pego et al., 2000).

One of the main advantages of ProteomeLab PF2D is its ability to give a global overview of protein levels in response to any given biotic or abiotic condition. This system was able to identify proteins encoded by genes identified in the gene expression profiling study. The correlation of proteomic and transcriptomic data demonstrates that the proteins identified were truly differentially expressed in response to *B. cinerea* infection. However, the proteome study also identified proteins encoded by genes not identified in the gene expression profiling study such as ascorbate peroxidase (At1g07890). This protein was identified in fractions that displayed an increase in absorbance. Similarly, proteins encoded by genes not identified in the gene expression profiling study were identified in fractions that displayed a reduction in absorbance. Expression of these proteins may be regulated post-transcriptionally. Given these advantages, ProteomeLab PF2D is a useful tool in studying protein expression studies but with plants, a few adjustments are essential in order to exploit the potential of this system. For instance, it is necessary to deplete RuBisCO from crude protein extracts before first dimension separation either by use of fractionation techniques (Dubin and Rajaram, 1996) or by use of kits (McDonald and Linde, 2002). This will improve the identification of low abundance proteins. Second, optimization of the extraction protocol may also improve the number of proteins ready for identification by mass spectrometry, for example, a $MgSO_4$-based extraction protocol (Pirondinia et al., 2006) led to increased identification of proteins than the urea-based extraction protocol used in this study. However, the major drawback of this system was the inability to determine the number of proteins within a selected fraction and the level to which the individual proteins are changing. This problem can be overcome by using the isobaric tags for relative and absolute quantification (iTRAQ) reagent in which the detectable elements of the proteome can be identified and quantified (Yan and Chen, 2005). With this system, samples can also be multiplexed considerably, reducing the time necessary for an experiment to be carried out.

The 2D LC system ProteomeLab PF2D identified some proteins likely to be differentially expressed. Some of the identified proteins matched genes differentially expressed in the microarray study while others did not. Verification of proteins that did not match those identified in the microarray study would be needed to determine if those proteins are changing in expression. This information is essential because it could demonstrate post-transcription regulation of proteins, a crucial addition to the usual transcirptomic approaches.

ACKNOWLEDGEMENTS

This work was funded by the Rockefeller Foundation Grant (FS320303) to the USHEPiA programme at the University of Cape Town for JM, grants from the National Research Foundation to KD (GUN 2054221, FA2005021500010) and a University of Cape Town International Travel Grant to JM. The authors acknowledge Susan Slade of the Biological Mass Spectrometry and Proteomics Facility, University of Warwick for her excellent technical assistance.

REFERENCES

Al-Shahrour F, Daz-Uriarte R, Dopazo J (2004) FatiGO: a web tool for finding significant associations of gene ontology terms with groups of genes. Bioinformatics, 20: 578-580

Bach M, Schnitzler JP, Seitz HU (1993) Elicitor-induced changes in Ca^{2+} influx, K^+ efflux, and 4-hydroxybenzoic acid synthesis in protoplasts of *Daucus carota* L. Plant Physiol. 103: 407-412

Blom N, Sicheritz-Pontn T, Gupta R, Gammeltoft S, Brunak S (2004) Prediction of post-translational glycosylation and phosphorylation of proteins from the amino acid sequence. Proteomics, 4: 1633-1649

Bradford MM (1976). A rapid and sensitive method for quantitation of micro- gram quantities of protein utilizing the principle of protein-dye-binding. Anal. Biochem. 72: 248-254

Chang SF, El-Bayoumy K, Sinha I, Trushin N, Stanley B, Pittman B, Prokopczyk B (2007). 4-(Methylnitrosamino)-I-(3-Pyridyl)-1-Butanone Enhances the Expression of Apolipoprotein A-I and Clara Cell 17-kDa Protein in the Lung Proteomes of Rats Fed a Corn Oil Diet but not a Fish Oil Diet. Cancer Epidemiol. Biomarkers Prev. 16: 228-235

Chou HM, Bundock N, Rolfe SA, Scholes JD (2000). Infection of *Arabidopsis thaliana* leaves with *Albugo candida* (white blister rust) causes a reprogramming of host metabolism. Mol. Plant Pathol. 1: 99-113

Coleman JOD, Blake-Kalff MMA, Davies TGE (1997). Detoxification of xenobiotics by plants: chemical modification and vacuolar compartmentation. Trends Plant Sci. 2: 141-151

Dangl JL, Dietrich RA, Richberg MH (1996). Death don't have no mercy: Cell death programs in plant-microbe interactions. Plant Cell 8: 1793-1807.

Deighton N, Muckenschnabel I, Colmenares AJ, Collado IG, Williamson B (2001). Botrydial is produced in plant tissues infected by *Botrytis cinerea*. Phytochemistry, 57: 689-692

Denby KJ, Kumar P, Kliebenstein DJ (2004). Identification of *Botrytis cinerea* susceptibility loci in *Arabidopsis thaliana*. Plant J. 38: 473-486.

Dik AJ, Koning G, Kohl J (1999).Evaluation of microbial antagonists for biological control of *Botrytis cinerea* stem infection in cucumber and tomato. Eur. J. Plant Pathol. 105: 115-122

Droby S, Lichter A (2004). Post-harvest Botrytis infection: etiology, development and management. *In* Y Elad, B Williamson, P Tudzynski, N Delen, eds, Botrytis: biology, pathology and control. Kluwer Academic Publishers, Dordrecht, The Netherlands, pp. 349-367

Dubin HJ, Rajaram S (1996). Breeding disease-resistant wheats for tropical highlands and lowlands. Annu. Rev. Phytopathol. 34: 503-526

Elad Y, Evensen K (1995). Physiological aspects of resistance to

Botrytis cinerea. Phytopathology, 85: 637-643
Felix G, Regnass M, Boller T (1993). Specific perception of sub-nanomolar concentrations of chitin fragments by tomato cells: induction of extracellular alkalinization, changes in protein phosphorylation, and establishment of a refractory state. Plant J. 4: 307-316
Gomord V, Faye L (2004). Posttranslational modification of therapeutic proteins in plants. Curr. Opin. Plant Biol. 7: 171-181.
Gorg A, Obermaier C, Boguth G, Weiss W (1999).. Recent developments in two-dimensional gel electrophoresis with immobilized pH gradients: wide pH gradients up to pH 12, longer separation distances and simplified procedures. Electrophoresis, 20: 712-717
Govrin EM, Levine A (2000). The hypersensitive response facilitates plant infection by the necrotrophic pathogen *Botrytis cinerea*. Curr. Biol. 10: 751-757
Grove H, Færgestad EM, Hollung K, Martens H (2009). Improved dynamic range of protein quantification in silver-stained gels by modelling gel images over time. Electrophoresis, 30: 1856-1862
Gygi SP, Rochon Y, Franza BR, Aebersold R (1999). Correlation between protein and mRNA abundance in yeast. Mol. Cell. Biol. 19: 1720-1730
Hamler RL, Zhu K, Buchanan NS, Kreunin P, Kachman MT, Miller FR, Lubman DM (2004). A two-dimensional liquid-phase separation method coupled with mass spectrometry for proteomic studies of breast cancer and biomarker identification. Proteomics, 4: 562-577
Han Y, Joosten HJ, Niu W, Zhao Z, Mariano PS, McCalman MT, Van Kan JAL, Schaap PJ, Dunaway-Mariano D (2007). Oxaloacetate hydrolase: the C-C bond lyase of oxalate secreting fungi. J. Biol. Chem. 282: 9581-9590
He SY, Bauer DW, Collmer A, Beer SV (1994). Hypersensitive response elicited by Erwinia amylovora harpin requires active plant metabolism. Mol. Plant Microbe Interact. 7: 289-292
Ideker T, Thorsson V, Ranish JA, Christmas R, Buhler J, Eng JK, Bumgarner R, Goodlett DR, Aebersold R, Hood L (2001). Integrated genomic and proteomic analyses of a systematically perturbed metabolic network. Science 292: 929-934
Jang JC, Sheen J (1994). Sugar sensing in higher plants. Plant Cell, 6: 1665-1679
Kamoun S, Kamdar HV, Tola E, Kado CI (1992). Incompatible interactions between crucifers and *Xanthomonas campestris* involve a vascular hypersensitive response: Role of the hrpX locus. Mol. Plant Microbe Interact. 5: 22-23
Kern W, Kohlmann A, Wuchte C, Schnittger S, Schoch C, Mergenthaler S, Ratei R, Ludwig WD, Hiddemann W, Haferlach T (2003). Correlation of protein expression and gene expression in acute leukemia. Cytometry, 55B: 29-36
Klose J (1975). Protein mapping by combined isoelectric focusing and electrophoresis of mouse tissues. A novel approach to testing for induced point mutations in mammals. Humangenetik, 26: 231-243
Kwon SJ, Choi EY, Choi YJ, Ahn JH, Park OK (2006). Proteomics studies of post-translational modifications in plants. J. Exp. Bot. 57: 1547-1551
Lamb CJ, Dixon RA (1997). The oxidative burst in Plant Disease resistance. Annu. Rev. Plant Physiol. Plant Mol. Biol. 48: 251-275
Lareau LF, Green RE, Bhatnagar RS, Brenner SE (2004). The evolving roles of alternative splicing. Curr. Opin. Struct. Biol. 14: 273-282
Leroux P, Fritz R, Debieu D, Albertini C, Lanen C, Bach J, Gredt M, Chapeland F (2002). Mechanisms of resistance to fungicides in field strains of *Botrytis cinerea*. Pest Manag. Sci. 58: 876-888
Levine A, Tenhaken R, Dixon R, Lamb C (1994). H_2O_2 from the oxidative burst orchestrates the plant hypersensitive disease resistance response. Cell, 79: 583-593
Lodish H, Berk A, Matsudaira P, Kaiser AC, Krieger M, Scott PM, Zipursky SL, Darnell J (2004). Molecular cell biology, Ed 5. W.H. Freeman and Company, New York
Mann M, Hendrickson RC, Pandey A (2001). Analysis of proteins and proteomes by mass spectrometry. Annu. Rev. Biochem. 70: 437-473
Marrs KA (1996). The functions and regulation of glutathione S-transferases in plants. Annu. Rev. Plant Physiol. Plant Mol. Biol. 47: 127-158
McDonald BA, Linde C (2002). The population genetics of plant pathogens and breeding strategies for durable resistance. Euphytica, 124: 163-180
Michelmore RW (2003). The impact zone: genomics and breeding for durable disease resistance. Curr. Opin. Plant Biol. 6: 397-404
Mulema JMK (2008). Molecular characterization of the *Arabidopsis thaliana* - *Botrytis cinerea* Interaction. University of Cape Town, Cape Town, South Africa
Mulema JMK, Denby KJ (2011). Spatial and temporal transcriptomic analysis of the *Arabidopsis thaliana* - *Botrytis cinerea* interaction. Mol. Biol. Rep. DOI 10.1007/s11033-011-1185-4
Murphy AM, Holcombe LJ, Carr JP (2000). Characteristics of salicylic acid-induced delay in disease caused by a necrotrophic fungal pathogen in tobacco. Physiol. Mol. Plant Pathol. 57: 47-54
Patterson SD (2004). How much of the proteome do we see with discovery-based proteomics methods and how much do we need to see? Curr Proteomics, 1: 3-12
Patton WF (2002). Detection technologies in proteome analysis. J. Chromatogr. B Analyt. Technol. Biomed. Life Sci. 771: 3-31
Peck SC (2005). Update on proteomics in Arabidopsis. where do we go from here? Plant Physiol. 138: 591-599
Pego JV, Kortstee AJ, Huijser C, Smeekens SCM (2000). Photosynthesis, sugars, and the regulation of gene expression. J. Exp. Bot. 51: 407-416
Peleman JD, Van der Voort JR (2003). Breeding by design. Trends Plant Sci. 8: 330-334
Pirondinia A, Visiolia G, Malcevschia A, Marmirol N (2006). A 2-D liquid-phase chromatography for proteomic analysis in plant tissues. J. Chromatogr. B Analyt. Technol. Biomed. Life Sci. 833: 91-100
Reddy ASN (2007). Alternative splicing of pre-messenger RNAs in plants in the genomic era. Annu Rev Plant Biol 58: 267-294
Rensink WA, Buell CR (2005). Microarray expression profiling resources for plant genomics. Trends Plant Sci. 10: 603-609
Schouten A, Tenberge KB, Vermeer J, Stewart J, Wagemakers L, Williamson B, Van Kan L (2002). Functional analysis of an extracellular catalase of Botrytis cinerea. Mol. Plant Pathol. 3: 227-238
Sharon N, Lis H (2004). History of lectins: from hemagglutinins to biological recognition molecules. Glycobiology, 14: 53R-62R
Staats M, van Baarlen P, Van Kan JAL (2005). Molecular phylogeny of the plant pathogenic genus *Botrytis* and the evolution of host specificity. Mol. Biol. Evol. 22: 333-346
Stab MR, Ebel J (1987). Effects of Ca^{2+} on phytoalexin induction by fungal elicitors in soybean cells. Arch. Biochem. Biophys. 257: 416-423
Stamm S, Ben-Ari S, Rafalska I, Tang Y, Zhang Z, Toiber D, Thanaraj TA, Soreq H (2005). Function of alternative splicing. Gene, 344: 1-20
Tenberge KB, Beckedorf M, Hoppe B, Schouten A, Solf M, Von den Driesch M (2002). In situ localization of AOS in host-pathogen interactions. Microsc. Microanal. 8(2): 250-251
Tiedemann AV (1997). Evidence for a primary role of active oxygen species in induction of host cell death during infection of bean leaves with Botrytis cinerea. Physiol. Mol. Plant Pathol. 50: 151-166
Viswanathan S, Unlu M, Minden JS (2006). Two-dimensional difference gel electrophoresis. Nat. Protoc. 1: 1351-1358
Westermeier R, Marouga R (2005). Protein detection methods in proteomics research. Bioscience Rep. 25: 19-32
Willekens H, Chamnongpol S, Davey M, Schraudner M, Langebartels C, Van Montagu M, Inze D, Van Camp W (1997). Catalase is a sink for H_2O_2 and is indispensable for stress defence in C3 plants. EMBO J. 16: 4806-4816
Williamson B, Tudzynski B, Tudzynski P, van Kan JAL (2007). *B. cinerea*: the cause of the grey mould diseases. Mol. Plant Pathol. 8: 561-580
Yan W, Chen SS (2005). Mass spectrometry-based quantitative proteomic profiling. Brief Funct. Genomic Proteomic, 4: 1-12
Zhu H, Bilgin M, Snyder M (2003). Proteomics. Annu. Rev. Biochem. 72: 783-812
Zimmerli L, Stein M, Lipka V, Schulze-Lefert P, Somerville S (2004). Host and non-host pathogens elicit different jasmonate/ethylene responses in Arabidopsis. Plant J. 40: 633-646